The Astrophysical Journal, 621:537–544, 2005 March 1

WATER PRODUCTION RATES, ROTATIONAL TEMPERATURES, AND SPIN TEMPERATURES IN COMETS C/1999 H1 (LEE), C/1999 S4, AND C/2001 A2

N. Dello Russo
Department of Physics, Catholic University of America, Washington, DC 20064; and Laboratory for Extraterrestrial Physics, NASA Goddard Space Flight Center, Code 690, Greenbelt, MD 20771

B. P. Bonev
Ritter Astrophysical Research Center, Department of Physics and Astronomy, University of Toledo, Toledo, OH 43606; and Laboratory for Extraterrestrial Physics, NASA Goddard Space Flight Center, Code 690, Greenbelt, MD 20771

M. A. DiSanti and M. J. Mumma
Laboratory for Extraterrestrial Physics, NASA Goddard Space Flight Center, Code 690, Greenbelt, MD 20771

E. L. Gibb
Department of Physics, University of Notre Dame, Notre Dame, IN 46556

K. Magee-Sauer
Department of Chemistry and Physics, Rowan University, Glassboro, NJ 08028

and

R. J. Barber and J. Tennyson
Department of Physics and Astronomy, University College London, Gower Street, London WC1E 6BT, UK
Received 2004 September 10; accepted 2004 November 7

ABSTRACT

Water hot-band lines were detected in comets C/1999 H1 (Lee), C/1999 S4 (LINEAR), and C/2001 A2 (LINEAR) in the 2.9 μm spectral region using high-dispersion ($\lambda/\Delta\lambda \sim 2 \times 10^4$) infrared spectroscopy with NIRSPEC at the W. M. Keck Observatory. The density of H_2O emissions in this spectral region, the spectral coverage and resolution of NIRSPEC, and fluorescence models developed for these hot bands enabled the determination of H_2O production rates, rotational temperatures, and ortho-to-para ratios (OPRs) in these comets. Previous studies revealed clear diversity in the volatile organic chemistries of these comets, suggesting that they may have formed in different regions of the early solar nebula. The nuclear spin temperature of H_2O as derived from its OPR is another possible indicator of cometary formation temperature and region. Nuclear spin temperatures for H_2O were derived on one date in comet S4 and two dates in Lee and A2. Derived spin temperatures for H_2O in these comets are $\geq$30, 30^{+15}_{-6}, and 23^{+4}_{-3} K for S4, Lee, and A2, respectively. Measurements are consistent with a possible link between nuclear spin temperatures and volatile abundances, but studies of more comets and continued improvements in water hot-band fluorescence models are needed to more stringently test this.

Subject headings: comets: general — comets: individual (C/1999 S4, C/2001 A2, Lee (C/1999 H1)) — infrared: solar system — techniques: spectroscopic

1. BACKGROUND

Knowledge of the composition and structure of the cometary nucleus is essential for understanding the formation and evolution of volatile material within our solar system. An important focus of current research is the degree to which the composition of precometary ices varied with distance from the young Sun. Based on dynamical arguments it is believed that Oort Cloud comets formed in the giant planets' region of the nebula between 5 and 40 AU (see Oort 1950; Dones et al. 2005). Molecular abundances in the nebula both in the gas phase and on ice mantles critically depend on the temperature and thus would have varied significantly with distance from the Sun. In addition to temperature gradients, ices and gases in this region were subjected to differing degrees of radiation processing (specifically UV and X-ray). For these reasons, Oort Cloud comets are expected to possess a range in volatile abundances reflective of their chemically diverse formative regions.

Emerging observational evidence supports this diversity. The methanol abundance in comets shows a wide range (<0.2%–6% relative to H_2O), with Oort Cloud comets showing both the lowest (LINEAR C/1999 S4) and highest (Austin 1990 V, C/1996 B1) values in this range (Mumma 1997; Mumma et al. 2001a; Bockelée-Morvan et al. 2001; Biver et al. 2002). Similar diversity is seen in the abundances of hypervolatiles CO (~1%–15% for the native ice; Feldman et al. 1997; DiSanti et al. 2001, 2003; Mumma et al. 2003) and CH_4 (~0.2%–1.5%; Gibb et al. 2003).

Water is the dominant ice in comets, so in the context of the overall volatile chemistry, it is important to accurately determine H_2O production rates. We have developed a technique for directly measuring gas-phase H_2O abundances in cometary comae from ground-based observatories based on infrared nonresonance (hot-band) fluorescence. Since hot-band emissions radiate to vibrational levels that lie well above the ground state, they are in general not strongly extinguished by terrestrial water. Thus, observing these transitions requires no specific cometary Doppler shift. This method has been routinely used to directly detect and determine H_2O production rates in comets for about the last 10 years (Mumma et al. 1995, 1996, 2001a, 2001b; Dello Russo et al. 2000, 2002a, 2002b, 2004; Weaver et al. 1999a, 1999b; Brooke et al. 2003).

TABLE 1
OBSERVING CIRCUMSTANCES

UT Date	R (AU)	Δ (AU)	Δ_{dot} (km s^{-1})	Setting[a]	ν_c[b] (cm^{-1})	$\lambda/\Delta\lambda$	AWV[c]	I_{time}[d] (minutes)	Lines Used[e]
C/1999 H1 (Lee)									
1999 Aug 19.6	1.049	1.381	−28.4	KL_1	3364.2	2.5×10^4	4.52	8	33 (10)
	...	...	...	KL_2	3408.9	...	...	10	...
	...	...	...	KL_3	3457.3	...	...	8	...
1999 Aug 21.6	1.076	1.348	−29.0	KL_1	3370.0	2.5×10^4	3.87	24	25 (10)
	...	...	...	KL_2	3439.8	...	...	24	...
C/1999 S4 (LINEAR)									
2000 Jul 13.6	0.804	0.546	−54.9	KL_1	3370.6	1.5×10^4	19.3	16	8 (3)
	...	...	...	KL_2	3442.2	...	...	28	...
C/2001 A2 (LINEAR)									
2001 Jul 9.5	1.160	0.275	11.4	KL_1	3368.8	2.5×10^4	7.55	20	17 (6)
	...	...	...	KL_2	3429.0	...	...	28	...
2001 Jul 10.5	1.173	0.282	12.4	KL_1	3368.7	2.5×10^4	8.06	16	17 (6)
	...	...	...	KL_2	3428.9	...	...	40	...
2001 Aug 4.4	1.510	0.578	25.9	KL_2	3428.7	2.5×10^4	3.24	12	9[f]
2001 Aug 10.5	1.594	0.673	28.0	KL_2	3428.9	2.5×10^4	3.85	20	10[f]

[a] NIRSPEC is cross-dispersed, so each setting samples multiple orders. All water lines used in this study are within order 26.
[b] The central wavenumber of the order (each setting encompasses ~50 cm^{-1} per order near 2.9 μm).
[c] The column burden of atmospheric water vapor in precipitable millimeters.
[d] On-source integration time.
[e] Total number of H_2O lines used in the analysis (see Table 2 and § 3). Emissions that are a blend of more than one rovibrational water line are counted only once. The number of para lines used in the analysis is given in parentheses after the number of total lines used.
[f] Emissions were co-added instead of analyzed individually.

The H_2O molecule is organized into distinct species according to whether the nuclear spin vectors of the hydrogen atoms are parallel (ortho ladder, $I = 1$) or antiparallel (para ladder, $I = 0$). The lowest ortho level lies 23.8 cm^{-1} (~34 K) above the lowest para level, so the ortho-to-para ratio (OPR) of H_2O is temperature-dependent. The OPR achieves the statistical equilibrium value of 3/1 for temperatures above ~50 K, whereas para states are increasingly favored at lower temperatures.

Once water molecules form, there is evidence that radiative and collisional processes are unlikely to cause conversion between spin states, so conversion times are thought to be very long. Theoretical studies demonstrate a radiative conversion time for H_2 (~10^{20} s) exceeding the age of the universe, and laboratory studies determined a collisional half-life of ~2×10^{17} collisions, or about 3 yr at standard temperature and pressure (see Farkas 1935; Dodelson 1986; Mumma et al. 1993). Laser-induced fluorescence studies of H_2O itself show no evidence of nuclear spin state conversion during molecular collisions (Nela et al. 2000). Nuclear spin conversion can occur faster in other molecules (e.g., CH_4; see Frayer & Ewing 1967); however, recent evidence suggests long nuclear spin conversion times for H_2O that are more analogous to H_2 than CH_4 (Miani & Tennyson 2004).

It is possible that nuclear spin conversion times for H_2O will be better constrained in the near future. It has been known for some time that nuclear spin conversion may occur between ortho and para rotational levels close in energy via hyperfine nuclear spin-rotational or spin-spin interactions (Curl et al. 1967). Recently, it has been suggested that this type of conversion could be observed experimentally, enabling the eventual development of a reliable nuclear spin conversion model for H_2O (Miani & Tennyson 2004).

Based on our knowledge to date, it is likely that H_2O molecules do not undergo nuclear spin conversion during their long residence in the comet nucleus or after sublimation into the coma prior to photodissociation. Thus, nuclear spin temperatures (derived from measured OPRs in the coma) may be a measure of the chemical formation temperature of water in comets and could provide clues about the formation region and processing histories of cometary ices (Mumma et al. 1989, 1993). Measurements of H_2O OPRs in comets were initially made in 1P/Halley and C/1986 P1 (Wilson) from the Kuiper Airborne Observatory. OPR = 2.5 ± 0.1, equivalent to a spin temperature of 29 K, was derived for comet Halley (Mumma et al. 1987, 1989, 1993). Comet Wilson, however, showed an OPR = 3.2 ± 0.2, which is consistent with statistical equilibrium at a spin temperature greater than 50 K (Mumma et al. 1989). The *Infrared Space Observatory* (*ISO*) observed the 2.6–2.9 μm spectral region, which contains bands of H_2O (ν_3, ν_1, and hot bands) in comets C/1995 O1 (Hale-Bopp) and 103P/Hartley 2 (Crovisier et al. 1997, 1999). The spectral resolution was sufficient ($\lambda/\Delta\lambda \sim 1500$) to resolve the stronger rovibrational lines. Based on *ISO* results, OPR = 2.45 ± 0.10 and 2.7 (corresponding to $T_{spin} = 28$ and 35 K) were determined for Hale-Bopp and Hartley 2, respectively. These results confirm that H_2O in comets can have spin temperatures of less than 50 K.

Studies of H_2O hot bands from ground-based observatories have the potential for more routine measurements of OPRs in comets. The targeting of hot bands and the use of sensitive high-resolution ($\lambda/\Delta\lambda \sim 2 \times 10^4$) ground-based spectrometers enables the detection of multiple rovibrational lines. Here we determine H_2O production rates, rotational temperatures, and OPRs for three Oort Cloud comets [C/1999 H1 (Lee), C/1999

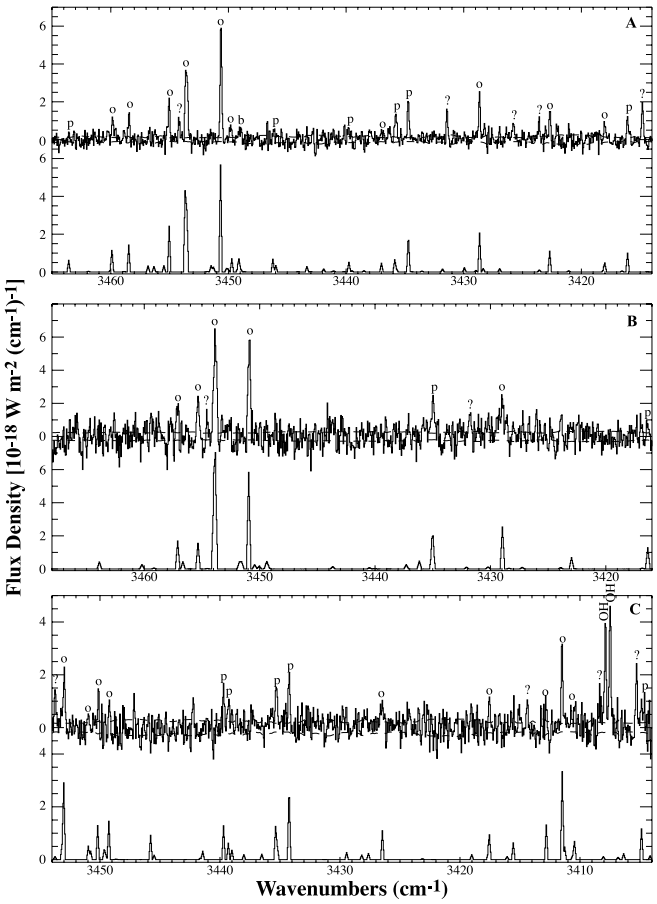

FIG. 1.—Comparison of spectral residuals for comets C/1999 H1 (Lee), C/1999 S4, and C/2001 A2 with best-fit fluorescence models. (*a*) *Top*: Spectral residuals for comet Lee on UT 1999 August 21.6, KL_2 setting (see Table 1). *Bottom*: H_2O fluorescence model (*solid curve*) for $Q_{H_2O} = 1.43 \times 10^{29}$ s^{-1}, $T_{rot} = 76$ K, and OPR = 2.3, convolved to the approximate resolution of the Lee comet residuals. (*b*) *Top*: Spectral residuals for comet C/1999 S4 on UT 2000 July 13.6, KL_2 setting (see Table 1). *Bottom*: H_2O fluorescence model (*solid curve*) for $Q_{H_2O} = 6.73 \times 10^{28}$ s^{-1}, $T_{rot} = 73$ K, and OPR = 2.8, convolved to the approximate resolution of the S4 comet residuals. (*c*) *Top*: Spectral residuals for comet C/2001 A2 on UT 2001 July 10.5, KL_2 setting (see Table 1). *Bottom*: H_2O fluorescence model (*solid curve*) for $Q_{H_2O} = 4.30 \times 10^{28}$ s^{-1}, $T_{rot} = 105$ K, and OPR = 1.8, convolved to the approximate resolution of the A2 comet residuals. Water hot-band lines are labeled "o" for ortho, "p" for para, and "b" for a blend of ortho and para. Unknown emission features are labeled with a question mark, and emissions due to OH are labeled in (*c*). The dashed curves superposed on the comet residuals are the ± 1 σ (photon) noise level.

S4 (LINEAR), and C/2001 A2 (LINEAR)]. Derived H_2O OPRs and volatile abundances in these comets are compared and discussed.

2. OBSERVATIONS AND DATA ANALYSIS

Observations were performed with the NIRSPEC spectrometer (McLean et al. 1998) at the 10 m W. M. Keck Observatory on Mauna Kea, Hawaii. The observing circumstances are summarized in Table 1. At each grating setting, comet data were acquired using a sequence of four scans (source, sky, sky, source). For sky spectra the telescope was nodded on the chip, providing sky cancellation via pixel-by-pixel subtraction. The source and sky frames are taken in positions approximately one-quarter the distance from the top and bottom of the slit, respectively (12″ nod along the slit). On-chip nodding allows more time on source to be obtained at the expense of spatial coverage. Flux calibrations were obtained for each grating/cross-disperser setting and were based on observations of standard stars through 3 and 5 pixel slits (corresponding to 0.″43 and 0.″72 slit widths, respectively), with corrections for slit losses included in our analysis.

The data were processed using algorithms specifically tailored to our comet observations. Application of these for data acquired with NIRSPEC has been described elsewhere (e.g., Mumma et al. 2001a, 2001b). Spectral frames were registered such that the spectral and spatial dimensions fell along rows and columns, respectively. Spectra were then extracted over any desired spatial extent and position along the slit. Atmospheric models were obtained using the Spectrum Synthesis Program (SSP; Kunde & Maguire 1974), which accesses the HITRAN-1992 Molecular Data Base (Rothman et al. 1992). SSP models were used to assign wavelength scales to the extracted spectra and to establish absolute column burdens for each significant absorbing species in the terrestrial atmosphere. The detectability of emission lines near 2.9 μm is particularly sensitive to the atmospheric water burden, which was notably high for S4 and A2 in July (Table 1).

Volatile emission features were separated from the continuum by subtracting the normalized atmospheric model from the comet spectrum row by row, yielding the net cometary molecular emission intensities along the slit (still convolved with the atmospheric transmittance function; see Fig. 1). The true line flux (F_{line}) incident at the top of the terrestrial atmosphere was determined by dividing the observed flux by the monochromatic transmittance (obtained from the fully resolved SSP model) at the Doppler-shifted line position. In this study, multiple lines from six different hot bands near 2.9 μm were detected.

3. RESULTS AND DISCUSSION

In order to obtain the rotational temperature, production rate, and OPR from measured line fluxes, the fluorescence efficiencies (g-factors) for individual rovibrational lines are needed as a function of temperature. We have developed fluorescence models for seven hot bands in the 2.9 μm region based on the methodology discussed in Dello Russo et al. (2000, 2004). Figure 1 shows a comparison of best-fit fluorescence models to spectral residuals of comets Lee, S4, and A2. In this work, lines from six hot bands were detected near 2.9 μm. The vibrational assignments for these six bands are 101–001 (corresponding to $\nu_1+\nu_3-\nu_3$), 101–100, 200–100, 200–001, 110–010, and 111–110.

Uncertainties in determining g-factors for these H_2O hot-band lines are discussed in detail elsewhere (Dello Russo et al. 2004). One problem is that laboratory measurements of absorption line strengths are not generally available for upward transitions from vibrationally excited states with energies higher than ν_2 (excitation energies exceed 4500 K for the next highest levels [020, 100, and 001], making it difficult to populate them significantly in the laboratory). Therefore, theoretical calculations were performed using first-principles variational nuclear motion calculations to determine Einstein A-coefficients. Energy levels and wave functions were calculated using program DVR3D (Tennyson et al. 2004) and the recent, spectroscopically determined, potential energy surface of Shirin et al. (2003). Einstein A-coefficients were then calculated using these wave functions and the ab initio dipole surface of A. E. Lynas-Gray et al. (2005, in preparation). These calculations used very highly converged wave functions, since they are part of a much more

extensive study designed for modeling the spectrum of hot water. The full calculations will be reported elsewhere.

Although Einstein A-coefficients were not determined in the laboratory, comets themselves may be used as ad hoc laboratories to test and improve the hot-band fluorescence models. Table 2 lists the specific emission lines (single and blended) used in this analysis. For each comet on each date, the individual fluxes from all measured lines were initially used in determining rotational temperatures and OPRs. Production rates were determined for each line individually based on the initially measured rotational temperature and OPR. Lines that gave systematically deviant production rates (i.e., higher or lower than the mean, at the 90% confidence level [Hoel 1984] averaged over at least three separate measurements of the line) were excluded from the analysis, while lines for which there were less than three separate measurements were always included (Table 2). Four lines were excluded for S4 and Lee on all dates, and three lines were excluded on the July dates for A2. No lines were excluded in the August A2 analysis (Table 2). Production rates, rotational temperatures, and OPRs were then recalculated (excluding deviant lines) for all comets and on all dates (Table 3).

The presence of systematically deviant lines suggests errors in the rotational branching ratios in the fluorescence models (derived production rates that were systematically high could also be caused by blending with unknown emissions). Improvements in dipole surface calculations are ongoing (A. E. Lynas-Gray et al. 2005, in preparation) and should reduce uncertainties in the hot-band fluorescence models in the future. As more high-resolution infrared measurements of these H_2O lines are obtained, systematically deviant emissions can be identified to help improve fluorescence models.

3.1. *Rotational Temperatures*

Knowledge of the rotational temperature (T_{rot}) is needed to determine total production rates from individual line intensities. We estimate T_{rot} in the ground vibrational level by comparing the transmittance-corrected H_2O line fluxes (F_{line}) with their calculated temperature-dependent g-factors (g_{line}), using all measured lines in the 2.9 μm region. At the correct rotational temperature, the quantity $F_{line}/(\nu_{line} g_{line})$ should be independent of the average energy of the lower state of the transition (as weighted by their relative contributions to the upper state population) for all measured lines (where ν_{line} is the line frequency in cm^{-1}). Additional details regarding determination of T_{rot} are given in Dello Russo et al. (2004).

The rotational temperature was measured on two dates for comets Lee and A2 and on one date for comet S4 (results are summarized in Table 3). Rotational temperatures were measured within apertures centered on the nucleus and correspond to an "average" over the region of the coma sampled by the aperture (Table 3). We note that gas rotational temperature is expected to vary in the coma with distance from the nucleus (Bockelée-Morvan 1987); however, the signal-to-noise ratio of individual H_2O lines was insufficient to accurately determine T_{rot} for off-nucleus extracts.

The ability to sample multiple lines with a wide range of ground-state rotational energies enabled accurate determinations of T_{rot}. Generally, the rotational temperature increases with increasing gas production rate and decreasing heliocentric distance (R_h). It is interesting to note the higher derived rotational temperature of H_2O in comet A2 (in July) compared to Lee and S4, despite a lower H_2O production rate and larger R_h. The meaning of the higher rotational temperature in A2 is unclear; however, we note that the aperture size at the comet (in km) was much smaller for A2 than for S4 and Lee (Table 3).

3.2. H_2O *Production Rates*

The methodology and examples for generating "Q-curves" and determining production rates have been discussed in detail in our previous work (Dello Russo et al. 1998, 2000, 2001, 2002b; Magee-Sauer et al. 1999, 2002; DiSanti et al. 2001). These studies clearly define the "nucleus-centered" and "terminal" (off-nucleus) production rates and the relation between them. For this work, production rates were determined within a nucleus-centered aperture (the size of the aperture is listed in Table 3). Since this "raw" nucleus-centered value underestimates the true production rate (Dello Russo et al. 1998), a correction factor based on the ratio of terminal to nucleus-centered production rates was applied. An accurate ratio can be obtained by summing all water lines within a grating setting and order and generating a Q-curve based on this sum. The ratio of terminal to nucleus-centered production rates from this Q-curve provides a correction factor by which the nucleus-centered Q for each line within a grating setting and order can be multiplied (we assume a constant T_{rot} from the nucleus-centered to the terminal region). This method is assumed to be valid since all lines within a single grating setting will be equally affected by seeing, drift, and telescope defocusing. In grating settings with many weak lines, this technique has the advantage of obtaining higher signal-to-noise ratios for line-by-line production rates (compared with using the terminal Q for each line individually).

Production rates were determined on two dates for comet Lee, on one date for S4, and on four dates for A2 (Table 3). The derived water production rates are in agreement with those previously derived for comet Lee (on UT August 20.6; Mumma et al. 2001b) and higher than those derived for comet S4 (by $\sim$50%) based on two hot-band lines detected near 4.7 μm on the same date (UT July 13.63; Mumma et al. 2001a). The primary reason for this discrepancy in S4 is that a rotational temperature of 50 K was assumed for H_2O in Mumma et al. (2001b). When the rotational temperature derived from this work (73 K) is applied to the lines analyzed in Mumma et al. (2001b), the production rates agree within error.

We note that in some cases, substantial differences exist between our derived water production rates and those derived by other techniques. Our revised water production rates for S4 are more than a factor of 2 higher than those inferred from observations of OH and H Lyα close to the time of our observations (Farnham et al. 2001; Mäkinen et al. 2001). Our water production rates for A2 are consistent with those obtained from the *Odin* satellite over a range of dates just prior to our observations (Lecacheux et al. 2003), but are about a factor of 5 lower than those inferred from *FUSE* observations starting UT 2001 July 12.6 (Feldman et al. 2002). Disagreement with *FUSE* production rates is not surprising since the *FUSE* results likely reflect increased comet activity due to an outburst on July 12 (Kysely et al. 2001; Morris et al. 2001). H_2O production rates were determined in comet Lee using *SWAS*, but they are not directly comparable to our results since measurements were obtained at different times (Neufeld et al. 2000; Chiu et al. 2001).

The differences between water production rates determined from different spectral regions (and different instruments, telescopes, etc.) impose problems that are not completely understood. As pointed out by Magee-Sauer et al. (1999), intercomparisons between results obtained from different

TABLE 2

H_2O Lines Analyzed near 2.9 μm

Rest Frequency (cm^{-1})	Vibrational Assignment	Rotational Assignment	Nuclear Spin Species	Dates Detected (UT)		
				Lee	S4	A2
3347.907.....	101–001	2_{20}–3_{31}	Ortho	1999 Aug 19.6, 21.6	None	None
3348.355.....	200–001	3_{22}–4_{23}	Para	1999 Aug 19.6, 21.6	None	None
3358.922.....	200–001	3_{03}–4_{04}	Ortho	1999 Aug 19.6, 21.6	None	2001 Jul 9.5, 10.5
3360.990.....	200–001	3_{13}–4_{14}	Para	None	None	2001 Jul 9.5, 10.5
3362.310.....	101–001	2_{12}–3_{21}	Para	1999 Aug 19.6, 21.6	None	None
3366.554.....	200–100	3_{22}–4_{31}	Para	1999 Aug 19.6, 21.6	None	None
3371.692.....	200–100	3_{13}–4_{22}	Para	1999 Aug 19.6, 21.6	2000 Jul 13.6	None
3372.754[a]	200–001	2_{21}–3_{22}	Ortho	1999 Aug 19.6, 21.6	2000 Jul 13.6	2001 Jul 9.5, 10.5
3378.484[a]	200–001	2_{02}–3_{03}	Para	1999 Aug 19.6, 21.6	None	2001 Jul 9.5, 10.5
3382.100.....	200–001	2_{12}–3_{13}	Ortho	1999 Aug 19.6, 21.6	2000 Jul 13.6	2001 Jul 9.5, 10.5
3387.541[a]	101–001	4_{04}–5_{15}	Ortho	1999 Aug 19.6, 21.6	2000 Jul 13.6	2001 Jul 9.5, 10.5
3390.017[a*]	101–100	2_{12}–3_{31}	Para	1999 Aug 19.6, 21.6	2000 Jul 13.6	None
3390.039[a*]	200–001	4_{14}–4_{13}	Ortho	...	...	...
3390.092[a*]	101–001	4_{14}–5_{05}	Para	...	...	...
3394.076.....	200–100	2_{21}–3_{30}	Ortho	1999 Aug 19.6	None	None
3397.628.....	101–001	1_{11}–2_{20}	Ortho	1999 Aug 19.6	None	None
3399.368.....	200–001	1_{01}–2_{02}	Ortho	1999 Aug 19.6	None	None
3404.243.....	101–001	1_{10}–2_{21}	Para	1999 Aug 19.6	None	None
3404.997.....	101–001	3_{03}–4_{14}	Para	1999 Aug 19.6	None	2001 Jul 9.5, 10.5, Aug 4.4, 10.5
3409.203.....	110–010	3_{30}–4_{41}	Ortho	1999 Aug 19.6	None	None
3410.577.....	101–100	6_{24}–7_{25}	Ortho	None	None	2001 Jul 9.5, 10.5
3411.613.....	101–001	3_{13}–4_{04}	Ortho	1999 Aug 19.6	None	2001 Jul 9.5, 10.5, Aug 4.4, 10.5
3412.924.....	200–100	2_{12}–3_{21}	Ortho	1999 Aug 19.6	None	2001 Jul 9.5, 10.5, Aug 4.4, 10.5
3415.699.....	101–100	3_{03}–4_{22}	Para	1999 Aug 19.6, 21.6	2000 Jul 13.6	2001 Aug 4.4, 10.5
3417.659*	200–100	3_{12}–4_{23}	Ortho	1999 Aug 19.6, 21.6	None	2001 Jul 9.5, 10.5
3417.775*	101–001	3_{22}–4_{13}	Ortho	...	...	...
3422.329.....	101–001	2_{02}–3_{13}	Ortho	1999 Aug 19.6, 21.6	None	None
3426.582.....	101–100	6_{15}–7_{16}	Ortho	None	None	2001 Jul 9.5, 10.5
3428.303.....	200–001	2_{12}–2_{11}	Ortho	1999 Aug 19.6, 21.6	2000 Jul 13.6	None
3434.330*	200–100	2_{11}–3_{22}	Para	1999 Aug 19.6, 21.6	2000 Jul 13.6	2001 Jul 9.5, 10.5, Aug 4.4, 10.5
3434.382*	101–100	4_{14}–4_{31}	Para	...	...	...
3434.399*	101–001	2_{12}–3_{03}	Para	...	...	...
3435.490.....	200–001	3_{22}–3_{21}	Para	1999 Aug 19.6, 21.6	None	2001 Jul 9.5, 10.5
3436.633*	101–001	4_{04}–4_{13}	Ortho	1999 Aug 19.6, 21.6	None	None
3436.643*	101–100	5_{33}–6_{34}	Ortho	...	...	...
3439.423.....	101–001	1_{01}–2_{12}	Para	1999 Aug 21.6	None	2001 Jul 9.5, 10.5, Aug 4.4, 10.5
3439.826.....	200–001	1_{11}–1_{10}	Para	None	None	2001 Jul 9.5, 10.5, Aug 4.4, 10.5
3445.885.....	200–001	2_{20}–2_{21}	Para	1999 Aug 21.6	None	2001 Aug 4.4, 10.5
3448.722*	111–110	5_{15}–6_{16}	Ortho	1999 Aug 19.6, 21.6	None	None
3448.742*	101–100	6_{06}–7_{07}	Ortho	...	...	...
3448.829*	101–100	6_{16}–7_{17}	Para	...	...	...
3449.376.....	101–100	5_{24}–6_{25}	Ortho	1999 Aug 19.6, 21.6	None	2001 Jul 9.5, 10.5
3450.294.....	200–001	1_{10}–1_{11}	Ortho	1999 Aug 19.6, 21.6	2000 Jul 13.6	2001 Jul 9.5, 10.5, Aug 4.4, 10.5
3451.089.....	101–001	4_{13}–4_{22}	Ortho	1999 Aug 21.6	None	2001 Jul 9.5, 10.5
3453.154*	101–100	2_{02}–3_{21}	Ortho	1999 Aug 19.6, 21.6	2000 Jul 13.6	2001 Jul 9.5, 10.5, Aug 10.5
3453.300*	200–100	1_{10}–2_{21}	Ortho	...	...	...
3454.689.....	101–001	2_{11}–2_{20}	Ortho	1999 Aug 19.6, 21.6	2000 Jul 13.6	None
3456.445[a,b]	101–100	4_{22}–5_{23}	Ortho	None	2000 Jul 13.6	None
3458.117.....	101–001	0_{00}–1_{11}	Ortho	1999 Aug 19.6, 21.6	None	None
3459.493*	101–100	4_{31}–5_{32}	Ortho	1999 Aug 19.6, 21.6	None	None
3459.529*	101–001	1_{11}–2_{02}	Ortho	...	...	...
3463.196†	200–100	3_{22}–3_{31}	Para	1999 Aug 19.6, 21.6	None	None
3463.234†	200–100	3_{13}–4_{04}	Para	...	...	...
3467.676.....	101–100	4_{13}–5_{14}	Ortho	1999 Aug 19.6	None	None
3468.532*	101–001	2_{02}–2_{11}	Ortho	1999 Aug 19.6	None	None
3468.631*	101–100	5_{05}–6_{06}	Para	...	...	...
3468.652*	200–001	1_{01}–0_{00}	Ortho	...	...	...
3468.754*	111–110	3_{12}–4_{13}	Para	...	...	...
3468.870*	101–100	5_{15}–6_{16}	Ortho	...	...	...
3472.285†	200–100	4_{32}–5_{23}	Ortho	1999 Aug 19.6	None	None
3472.357†	111–110	3_{22}–4_{23}	Ortho	...	...	...

Note.—Asterisks (*) or daggers (†) indicate emissions that are combinations of two or more lines.

[a] Lines excluded from the analysis for all comets on all dates (see § 3).

[b] This line was detected and analyzed on three dates in comet 153P/Ikeya-Zhang (C/2002 C1) and was suspected of being a blended emission (Dello Russo et al. 2004), so it was excluded from this analysis since there are four total measurements of this line in our comet data archive (see text).

TABLE 3

T_{rot}, Ortho-to-Para Ratio, and Q_{H_2O} for Comets Lee, S4, and A2

UT Date	R (AU)	Δ (AU)	Aperture Size[a]	T_{rot}[b] (K)	OPR[b]	T_{spin}[b] (K)	Q_{H_2O}[b,c]
C/1999 H1 (Lee)							
1999 Aug 19.6	1.049	1.381	420 × 1710	80^{+6}_{-4}	2.5 ± 0.5	≥23	13.35 ± 1.28
	...	...	...	80^{+15}_{-9}	2.5 ± 1.2	≥17	13.35 ± 2.58
1999 Aug 21.6	1.076	1.348	410 × 1670	76^{+4}_{-3}	2.5 ± 0.5	≥23	14.31 ± 1.33
	...	...	...	76^{+10}_{-6}	2.5 ± 1.1	≥18	14.31 ± 2.71
C/1999 S4 (LINEAR)							
2000 July 13.6	0.804	0.546	290 × 680	73^{+8}_{-6}	2.8 ± 0.3	≥30	6.73 ± 0.56
	...	...	...	73^{+19}_{-12}	2.8 ± 1.4	≥18	6.73 ± 1.19
C/2001 A2 (LINEAR)							
2001 July 9.5	1.16	0.275	84 × 340	98^{+6}_{-5}	2.5 ± 0.4	30^{+15}_{-6}	3.77 ± 0.34
	...	...	...	98^{+13}_{-8}	2.5 ± 1.0	≥19	3.77 ± 0.71
2001 July 10.5	1.173	0.282	86 × 350	105^{+5}_{-3}	1.8 ± 0.2	21 ± 2	4.30 ± 0.37
	...	...	...	105^{+12}_{-7}	1.8 ± 0.6	21^{+7}_{-4}	4.30 ± 0.76
2001 Aug 4.4	1.510	0.578	180 × 720	70[d]	2.1[d]	...	1.09 ± 0.17
2001 Aug 10.5	1.594	0.673	210 × 830	70[d]	2.1[d]	...	0.62 ± 0.14

[a] The aperture size in km (columns × rows) at the comet where T_{rot}, OPR, and Q_{H_2O} were determined. These extracts were centered on the nucleus. In units of pixels the extracts are 3×9 for comets Lee and A2, and 5×9 for comet S4. In units of arcseconds $3 \times 9 = 0''.42 \times 1''.74$ and $5 \times 9 = 0''.72 \times 1''.74$.

[b] For T_{rot}, OPR, T_{spin}, and Q_{H_2O}, the error bars for the upper values in these cells represent standard errors, and the error bars for the lower values in these cells represent the 95% confidence level (e.g., Arkin & Colton 1970; Hoel 1984). For A2 in August, the errors bars in Q_{H_2O} represent the standard errors. The weighted average of OPRs on August 19.6 and 21.6 in Lee gives an average spin temperature of 30^{+15}_{-6} K (standard error). The weighted average of OPRs on July 9.5 and 10.5 in A2 gives an average spin temperature of 23^{+4}_{-3} K (standard error).

[c] The water production rate × 10^{28} molecules s^{-1}.

[d] Assumed rotational temperature or OPR. Assumed OPRs are based on a weighted average derived on UT 2001 July 9.5 and 10.5. Assumed rotational temperatures are based on T_{rot} derived for HCN in A2 on UT 2001 August 4.4 (K. Magee-Sauer et al. 2005, in preparation).

techniques may be misleading. Agreement between absolute production rates may in some cases be more coincidental than consistent because the various methods are subject to widely different observational approaches, beam sizes, (not always understood) systematic effects, and modeling assumptions and complexity. Simultaneous measurements of different species (as is the case with data obtained with NIRSPEC) can help eliminate some systematic errors.

3.3. *Ortho-to-Para Ratio*

A sufficient number of both ortho and para lines were detected (see Tables 1 and 2) to determine OPRs for comets Lee and A2 on two dates and for S4 on one date (Table 3). These OPRs represent an average in the coma within the given aperture size (see Table 3). The derived nuclear spin temperatures of water released from comets A2, Lee, and S4 are respectively 23^{+4}_{-3}, 30^{+15}_{-6}, and ≥30 K (from a weighted average of the two dates on which OPRs were measured in Lee and A2). Low spin temperatures measured in these comets suggest that their H_2O likely formed on cold grains (with T_{spin} reflecting grain temperatures), rather than from exothermic gas-phase reactions (Tielens & Allamandola 1987). Nuclear spin temperatures in comets A2 and Lee are much lower than derived rotational temperatures, suggesting that H_2O OPRs are not reset to the coma gas temperature upon sublimation from the nucleus. We note that optical depth effects could simulate low OPRs; however, relevant transitions are optically thin outside a few kilometers (at most) from the nucleus (Dello Russo et al. 2004).

Spin temperatures have also been derived for NH_3 (assuming that NH_2 originates solely from the photodissociation of NH_3) in comets A2 (25^{+1}_{-2} K; Kawakita et al. 2002, 2004) and S4 (27^{+3}_{-2} K; Kawakita et al. 2001, 2004). A comparison of these results shows a possible correlation between spin temperatures for H_2O and NH_3 (spin temperatures for H_2O and NH_3 are within error in A2 and S4). However, a comparison in more comets is needed to establish a relationship (if any) between spin temperatures for H_2O, NH_3, and other species.

We note that the smaller error bars reported in the aforementioned study are not directly comparable to ours because they were calculated in a self-consistent but different way. Kawakita et al. pointed out that they had used only the "reciprocal" errors (as determined solely from the error associated with each measurement; see, e.g., Bevington & Robinson 1992) in obtaining a mean OPR (and corresponding spin temperature) from two individual line measurements. The dominant error in our analysis is not the reciprocal error, but is instead the standard error of the mean (Bevington & Robinson 1992; Arkin & Colton 1970) for a given date. The standard error depends on the dispersion of the individual line measurements around their weighted mean value. While the reciprocal error usually reflects photon or background noise within spectral extracts, the standard error of the mean encompasses additional effects, such as model uncertainties and the influence of small-number statistics.

3.4. *Comparing Ortho-to-Para Ratios to Volatile Chemistries*

A comparison of water OPRs with volatile chemistries may provide insights into the formation region for ices in these

TABLE 4
A Comparison of Volatile Abundances and Spin Temperatures in Comets S4, Lee, and A2

Comet	Relative Abundances (% with Respect to H_2O)[a]						
	CO	CH_4	C_2H_6	CH_3OH	HCN	C_2H_2	T_{spin} (K)
S4[b]	0.28	0.14	0.11	<0.15	0.08	<0.12	≥30
Lee[c]	1.5	1.0	0.65	1.7	0.18	0.22	30^{+15}_{-6}[d]
A2[e]	~3.5	~0.9–2.7	~1.6	~4.0	~0.5	~0.4	23^{+4}_{-3}[d]

[a] All volatile mixing ratios obtained from previous work are updated to reflect water production rates derived from this work.
[b] Mixing ratios are for UT 2000 July 13.6. Volatile production rates from Mumma et al. (2001a), except for CH_4 (Gibb et al. 2003).
[c] Mixing ratios are for UT 1999 Aug 21.6, except for CO, which was measured on Aug 20.6. Volatile production rates from Mumma et al. (2001b), except for CH_4 (Gibb et al. 2003).
[d] Spin temperatures based on a weighted average of two dates.
[e] Mixing ratios for A2 are approximate. Date-by-date values for relative abundances in A2 are reported in K. Magee-Sauer et al. (2005, in preparation) and E. L. Gibb et al. (2005, in preparation).

comets. It has been argued that the volatile abundances in Oort Cloud comets likely reflect the region in the solar nebula where they formed (see Mumma et al. 2001a). These three comets show diverse volatile chemistries (Table 4), suggesting different formation regions. In particular, the depleted volatile abundances in S4 suggest its formation in a warm region of the nebula, perhaps near Jupiter (Mumma et al. 2001a), while enhanced abundances in A2 suggest its formation in a cold region of the nebula, perhaps near Neptune (K. Magee-Sauer et al. 2005, in preparation).

The derived nuclear spin temperatures are consistent with formation of H_2O in these comets in different regions of the solar nebula (perhaps consistent also with their different volatile chemistries). However, the results are not sensitive enough to rule out formation of H_2O in these comets at similar temperatures (near 30 K) in the nebula, or in the presolar molecular cloud before formation of the solar system. It is not clear from this study whether or not measured OPRs are correlated with volatile abundances or provide insight into the formative region of comets, but studies of more comets and continued improvements in H_2O hot-band fluorescence models are needed to more stringently test this.

4. SUMMARY

Production rates for H_2O were derived in comets C/1999 H1 Lee (2 dates), C/1999 S4 (1 date), and C/2001 A2 (4 dates) based on the detection of multiple hot-band lines near 2.9 μm with NIRSPEC at the W. M. Keck Observatory (Tables 2 and 3). Measurements of multiple lines having a range of lower state energies allowed the accurate determination of rotational temperatures in these three comets (Table 3). We note that the retrieved rotational temperatures were highest in comet A2, although for these measurements its H_2O production rate was the lowest, and it was at a larger heliocentric distance than Lee and S4. We also note that the geocentric distance of A2 was much smaller than for Lee or S4, so the region of the coma sampled for A2 was weighted closer to the nucleus (Table 3). Ortho-to-para ratios and associated nuclear spin temperatures for H_2O were determined in these comets (Table 3). The derived spin temperatures of water released from comets A2, Lee, and S4 are 23^{+4}_{-3}, 30^{+15}_{-6}, and ≥30 K, respectively. Thus our results are marginally consistent with the formation of H_2O in these comets in different regions of the solar nebula, suggesting a possible correlation between the H_2O nuclear spin temperatures and the diverse volatile abundances of these comets (Table 4). However, the sensitivity of our measurements is insufficient to rule out formation of water in these comets at similar temperatures (near 30 K) either in the nebula or in the presolar molecular cloud. As more comets are sampled and H_2O hot-band fluorescence models are improved, the connection between volatile chemistries, OPRs, and formation histories should become clearer.

This work was supported by the NASA OSS Planetary Atmospheres Program under NAG5-10795 and NAG5-12285 to N. D. R., and the Planetary Astronomy Program under RTOP 693-344-32-30-07 to M. J. M. J. T. and R. L. B. were supported for this work by PPARC. We acknowledge the UCL HiPerSPACE computer center, where calculations of Einstein *A*-coefficients were performed. We thank Ian McLean and David Sprayberry for acquiring data on comet A2 on UT 2001 August 4. We thank Hal Weaver for helpful comments on the manuscript. Data presented herein were obtained at the W. M. Keck Observatory, which is operated as a scientific partnership among the California Institute of Technology, the University of California, and the National Aeronautics and Space Administration. The Observatory was made possible by the generous financial support of the W. M. Keck Foundation. The authors wish to recognize and acknowledge the very significant cultural role and reverence that the summit of Mauna Kea has always had within the indigenous Hawaiian community. We are most fortunate to have the opportunity to conduct observations from this mountain.

REFERENCES

Arkin, H., & Colton, R. R. 1970, Statistical Methods (New York: Barnes & Noble)
Bevington, P. R., & Robinson, D. K. 1992, Data Reduction and Error Analysis for the Physical Sciences (New York: McGraw-Hill)
Biver, N., et al. 2002, Earth Moon Planets, 90, 323
Bockelée-Morvan, D. 1987, A&A, 181, 169
Bockelée-Morvan, D., et al. 2001, Science, 292, 1339
Brooke, T. Y., Weaver, H. A., Chin, G., Bockelée-Morvan, D., Kim, S. J., & Xu, L.-H. 2003, Icarus, 166, 167
Chiu, K., Neufeld, D. A., Bergin, E. A., Melnick, G. J., Patten, B. M., Wang, Z., & Bockelée-Morvan, D. 2001, Icarus, 154, 345
Crovisier, J., et al. 1997, Science, 275, 1904

Crovisier, J., et al. 1999, in The Universe as Seen by *ISO*, ed. P. Cox & M. F. Kessler (ESA SP-427; Noordwijk: ESA), 137
Curl, R. F., Jr., Kasper, J. V. V., & Pitzer, K. S. 1967, J. Chem. Phys., 46, 3220
Dello Russo, N., DiSanti, M. A., Magee-Sauer, K., Gibb, E., & Mumma, M. J. 2002a, in Proc. Asteroids, Comets, and Meteors—ACM 2002, ed. B. Warmbein (ESA SP-500; Noordwijk: ESA), 689
Dello Russo, N., DiSanti, M. A., Mumma, M. J., Magee-Sauer, K., & Rettig, T. W. 1998, Icarus, 135, 377
Dello Russo, N., Mumma, M. J., DiSanti, M. A., & Magee-Sauer, K. 2002b, J. Geophys. Res., 107(E11), 5095
Dello Russo, N., Mumma, M. J., DiSanti, M. A., Magee-Sauer, K., & Novak, R. 2001, Icarus, 153, 162
Dello Russo, N., Mumma, M. J., DiSanti, M. A., Magee-Sauer, K., Novak, R., & Rettig, T. W. 2000, Icarus, 143, 324
Dello Russo, N., et al. 2004, Icarus, 168, 186
DiSanti, M. A., Mumma, M. J., Dello Russo, N., Magee-Sauer, K., & Griep, D. M. 2003, J. Geophys. Res., 108(E6), 5061
DiSanti, M. A., Mumma, M. J., Dello Russo, N., Magee-Sauer, K., Novak, R., & Rettig, T. W. 2001, Icarus, 153, 361
Dodelson, S. 1986, J. Phys. B, 19, 2871
Dones, L., Weissman, P. R., Levison, H. F., & Duncan, M. J. 2005, in Comets II, ed. M. C. Festou, H. U. Keller, & H. A. Weaver (Tucson: Univ. Arizona Press), 153
Farkas, A. 1935, Orthohydrogen, Parahydrogen, and Heavy Hydrogen (New York: Cambridge Univ. Press)
Farnham, T. L., Schleicher, D. G., Woodney, L. M., Birch, P. V., Eberhardy, C. A., & Levy, L. 2001, Science, 292, 1348
Feldman, P. D., Festou, M. C., Tozzi, G. P., & Weaver, H. A. 1997, ApJ, 475, 829
Feldman, P. D., Weaver, H. A., & Burgh, E. B. 2002, ApJ, 576, L91
Frayer, F. H., & Ewing, G. E. 1967, J. Chem. Phys., 48, 781
Gibb, E. L., Mumma, M. J., Dello Russo, N., DiSanti, M. A., & Magee-Sauer, K. 2003, Icarus, 165, 391
Hoel, P. G. 1984, Introduction to Mathematical Statistics (New York: Wiley)
Kawakita, H., Watanabe, J., Fuse, T., Furusho, R., & Abe, S. 2002, Earth Moon Planets, 90, 371
Kawakita, H., et al. 2001, Science, 294, 1089
———. 2004, ApJ, 601, 1152
Kunde, V. G., & Maguire, J. C. 1974, J. Quant. Spectrosc. Radiat. Transfer, 14, 803
Kysely, J., Baroni, S., Hornoch, K., & Morris, C. S. 2001, IAU Circ., 7659, 2
Lecacheux, A., et al. 2003, A&A, 402, L55
Magee-Sauer, K., Mumma, M. J., DiSanti, M. A., & Dello Russo, N. 2002, J. Geophys. Res., 107(E11), 5096
Magee-Sauer, K., Mumma, M. J., DiSanti, M. A., Dello Russo, N., & Rettig, T. W. 1999, Icarus, 142, 498
Mäkinen, J. T., Bertaux, J.-L., Combi, M. R., & Quémerais, E. 2001, Science, 292, 1326
McLean, I. S., et al. 1998, Proc. SPIE, 3354, 566
Miani, A., & Tennyson, J. 2004, J. Chem. Phys., 120, 2732
Morris, C. S., Lehky, M., Pereira, A., Bouma, R. J., Hasubick, W., Spratt, C. E., & Terbacz, A. 2001, IAU Circ. 7676, 4
Mumma, M. J. 1997, in ASP Conf. Ser. 122, From Stardust to Planetesimals, ed. Y. Pendleton & A. G. G. M. Tielens (San Francisco: ASP), 369
Mumma, M. J., Blass, W. E., Weaver, H. A., & Larson, H. P. 1989, in Formation and Evolution of Planetary Systems, ed. H. A. Weaver & L. Danly (Cambridge: Cambridge Univ. Press), 157
Mumma, M. J., DiSanti, M. A., Dello Russo, N., Fomenkova, M., Magee-Sauer, K., Kaminski, C. D., & Xie, D. X. 1996, Science, 272, 1310
Mumma, M. J., DiSanti, M. A., Dello Russo, N., Magee-Sauer, K., Gibb, E., & Novak, R. 2003, Adv. Space Res., 31, 2563
Mumma, M. J., DiSanti, M. A., Tokunaga, A., & Roettger, E. E. 1995, BAAS, 27, 1144
Mumma, M. J., Weaver, H. A., & Larson, H. P. 1987, A&A, 187, 419
Mumma, M. J., Weissman, P. R., & Stern, S. A. 1993, in Protostars and Planets III, ed. E. H. Levy & J. I. Lunine (Tucson: Univ. Arizona Press), 1177
Mumma, M. J., et al. 2001a, Science, 292, 1334
———. 2001b, ApJ, 546, 1183
Nela, M., Permogorov, D., Miani, A., & Halonen, L. 2000, J. Chem. Phys., 113, 1795
Neufeld, D. A., et al. 2000, ApJ, 539, L151
Oort, J. H. 1950, Bull. Astron. Inst. Netherlands, 11, 91
Rothman, L. S., et al. 1992, J. Quant. Spectrosc. Radiat. Transfer, 48, 469
Shirin, S. V., Polyansky, O. L., Zobov, N. F., Barletta, P., & Tennyson, J. 2003, J. Chem. Phys., 118, 2124
Tennyson, J., Kostin, M. A., Barletta, P., Harris, G. J., Polyansky, O. L., Ramanlal, J., & Zobov, N. F. 2004, Comput. Phys. Commun., 163, 85
Tielens, A. G. G. M., & Allamandola, L. J. 1987, in Interstellar Processes, ed. D. J. Hollenbach & H. A. Thronson, Jr. (Dordrecht: Reidel), 397
Weaver, H. A., Brooke, T. Y., Chin, G., Kim, S. J., Bockelée-Morvan, D., & Davies, J. K. 1999a, Earth Moon Planets, 78, 71
Weaver, H. A., Chin, G., Bockelée-Morvan, D., Crovisier, J., Brooke, T. Y., Cruikshank, D. P., & Geballe, T. R. 1999b, Icarus, 142, 482